EARTH OBSERVATION – SECOND ASSIGNMENT

Surname and name: Rossini Valerio

1. **Download and install SNAP (if needed, you can use a Virtual Machine to exploit the resources available within ESA Cloud Toolbox facility at http://eogrid.esrin.esa.int/cloudtoolbox after registering)**

The Sentinel Application Platform (SNAP) reunites all Sentinel Toolboxes in order to offer the most complex platform for this mission. The basic function includes: opening a product, exploring the product components such as bands, masks and tie point grids. Navigation tools and pixel information functionality also represents some of the basic capabilities. After that we have downloaded SNAP, we can go the next point.

2. **Follow LearnEO-Lesson13 (http://www.learn-eo.org/lessons/l13), step by step as in the following, by using SNAP instead of Bilko tool**

Going in the site (http://www.learn-eo.org/lessons/l13), we can see that the lesson is divided into the following sections:

- Opening and examining SEVIRI data from the region of interest
- Opening and examining MODIS data from the region of interest
- Processing the data to create visible composite images
- Processing the data to build up an ash detection algorithm.

3. **Download the SEVIRI/METEOSAT and MODIS/AQUA imagery on the case study of the 2010 Icelandic eruption of 2010, following LearnEO-Lesson13 instructions or download data provided by the professor.**

We have chosen to download the SEVIRI/METEOSAT and MODIS/AQUA imagery on the case study of the 2010 Icelandic eruption of 2010, following LearnEO-Lesson13 instructions

The available data sets are the following:

- MSG_201005081200.zip
- MSG_201101122300.zip
- MOD02HKM.A2010129.1225.005.7z

The MSG system provides accurate weather monitoring data through SEVIRI, which has the capacity to observe the Earth in 12 spectral channels (in table 1, we can see these channels and the relative main applications).

The data provided by MSG's SEVIRI instrument supports a large range of nowcasting applications:

- Detailed monitoring of convection.
- The detection of fog, dust storms or ash.
- The assessment of air mass characteristics.

We are interested in the monitoring of the volcanic ash clouds, that is important - for example - for air traffic management.

Channel No.	Spectral Band (μm)	Main application
1	VIS0.6	Surface, clouds, wind fields
2	VIS0.8	Surface, clouds, wind fields
3	NIR1.6	Surface, cloud phase
4	IR3.9	Surface, clouds, wind fields
5	WV6.2	Water vapor, high level clouds, atmospheric instability
6	WV7.3	Water vapor, atmospheric instability
7	IR8.7	Surface, clouds, atmospheric instability
8	IR9.7	Ozone
9	IR10.8	Surface, clouds, wind fields, atmospheric instability
10	IR12.0	Surface, clouds, atmospheric instability
11	IR13.4	Cirrus cloud height, atmospheric instability
12	HRV	Surface, cloud phase

Table 1: Spectral channel characteristics of SEVIRI in terms of the main application areas of each channel.

4. Perform data quality check

For checking the data quality, we can affirm that:

- If we take the MODIS imaginary (MOD02HKM.A2010129.1225.005), we consider:
  - good images that derived from the following channels:
    - EV_250_Aggr500_RefSB.1
    - EV_250_Aggr500_RefSB.2
    - EV_500_RefSB.3
    - EV_500_RefSB.4
    - EV_500_RefSB.5
    - EV_500_RefSB.6
    - EV_500_RefSB_Uncert_Indexes.6
  - bad images that derived from the following channels:
    - EV_500_RefSB.7
    - EV_250_Aggr500_RefSB_Uncert_Indexes.1
    - EV_250_Aggr500_RefSB_Uncert_Indexes.2
    - EV_500_RefSB_Uncert_Indexes.3
    - EV_500_RefSB_Uncert_Indexes.4
    - EV_500_RefSB_Uncert_Indexes.5
    - EV_500_RefSB_Uncert_Indexes.7
    - EV_250_Aggr500_RefSB_Samples_Used.1
    - EV_250_Aggr500_RefSB_Samples_Used.2
- If we take the SEVIRI imaginary (MSG_201005081200), we consider:
  - good images that derived from the following channels:
    - VIS0.6
    - VIS0.8
    - NIR1.6
    - IR3.9
    - WV6.2
    - WV7.3
    - IR8.7
    - IR9.7

        - IR10.8
        - IR12.0
        - IR13.4
        - HRV
    - No failures/stripes
- If we take the SEVIRI imaginary (MSG_201005081300), we consider:
    - good images that derived from the following channels:
        - IR3.9
        - WV6.2
        - WV7.3
        - IR8.7
        - IR9.7
        - IR10.8
        - IR12.0
        - IR13.4
        - HRV
    - bad images that derived from the following channels:
        - VIS0.6
        - VIS0.8
        - NIR1.6

Below we have a comparison using the MODIS or SEVIRI imaginary:

- Comparison of a good image derived from the channel EV_250_Aggr500_RefSB.1 and a bad image derived from the channel EV_500_RefSB_Uncert_Indexes.7 (MOD02HKM.A2010129.1225.005)

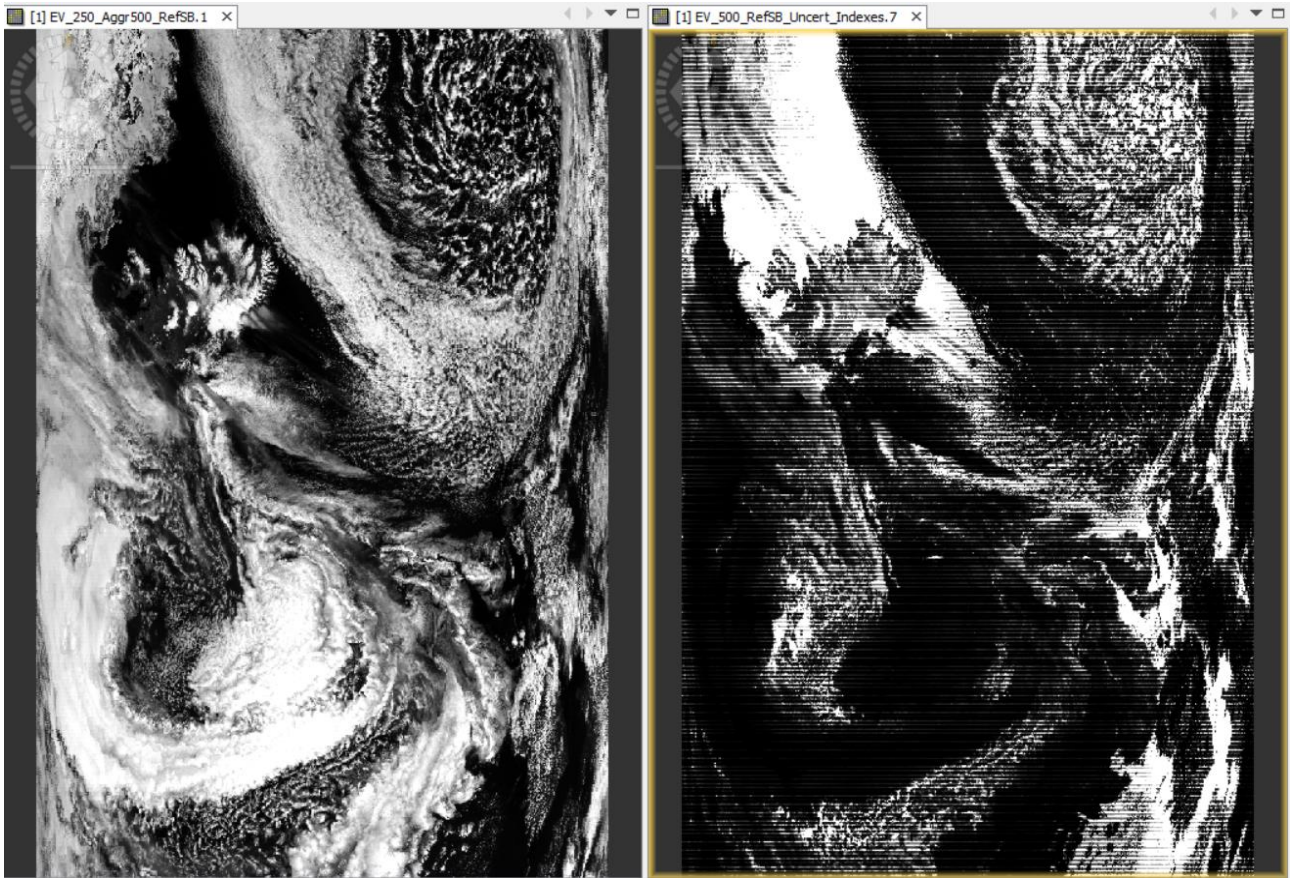

Figure 1: comparison of EV_250_Aggr500_RefSB.1 and EV_500_RefSB.7 using MOD02HKM.A2010129.1225.005

- Comparison of two good image derived from the channel VIS0.6 and the channel IR_016 (MSG_201005081200)

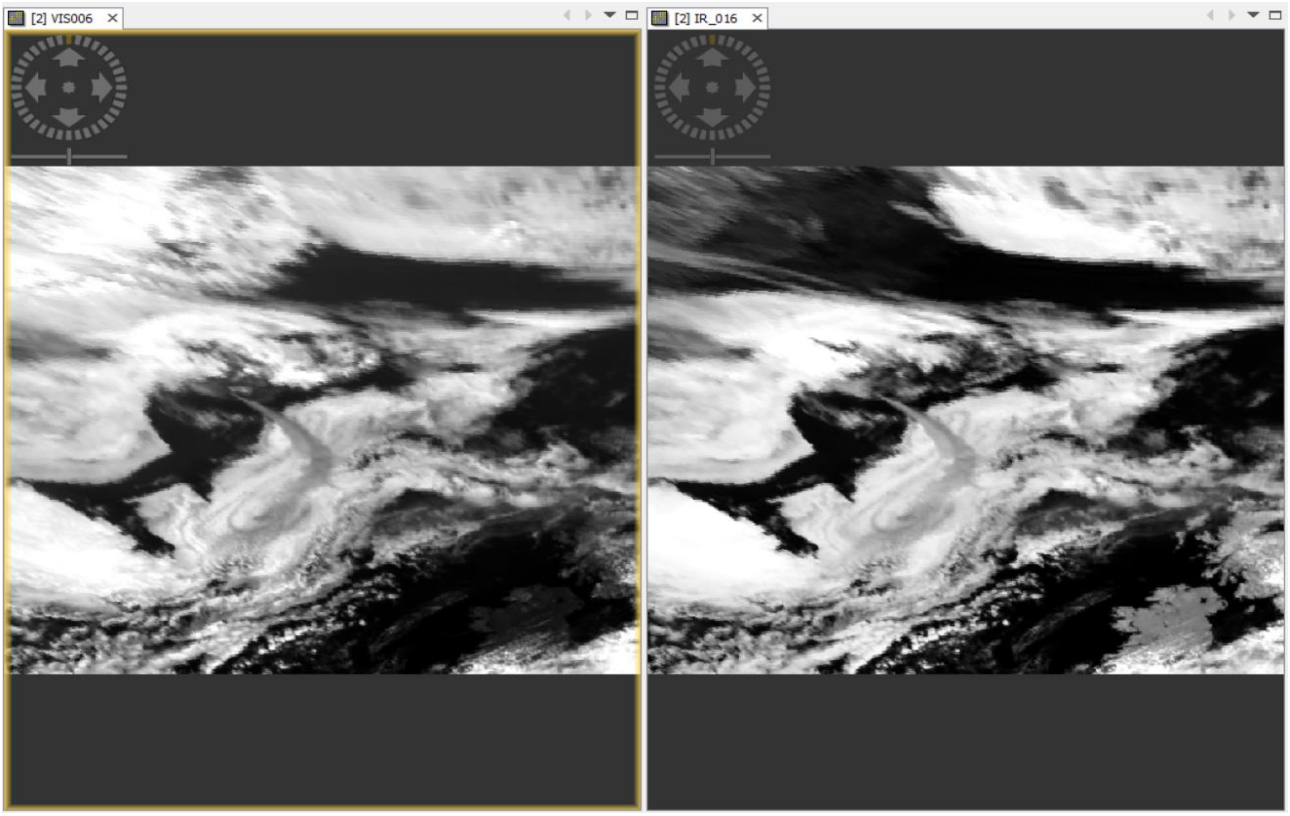

Figure 2: comparison of VIS0.6 and IR_016 using MSG_201005081200

- Comparison of a good image derived from the channel IR_039 and a bad image derived from the channel VIS0.6 (MSG_201005081300)

Figure 3: comparison of VIS0.6 and IR_016 using MSG_201005081300

5. Perform and display “visible” RGB (Red Green Blue) composite with MODIS data

For creating an RGB visible composite image, we have used:

- EV_250_Aggr1km_RefSB_1 (645 nm) – MODIS Band 1 [620-670 nm] RED
- EV_250_Aggr1km_RefSB_4 (555 nm) – MODIS Band 4 [545-565 nm] GREEN
- EV_250_Aggr1km_RefSB_3 (469 nm) – MODIS Band 3 [459-479 nm] BLUE

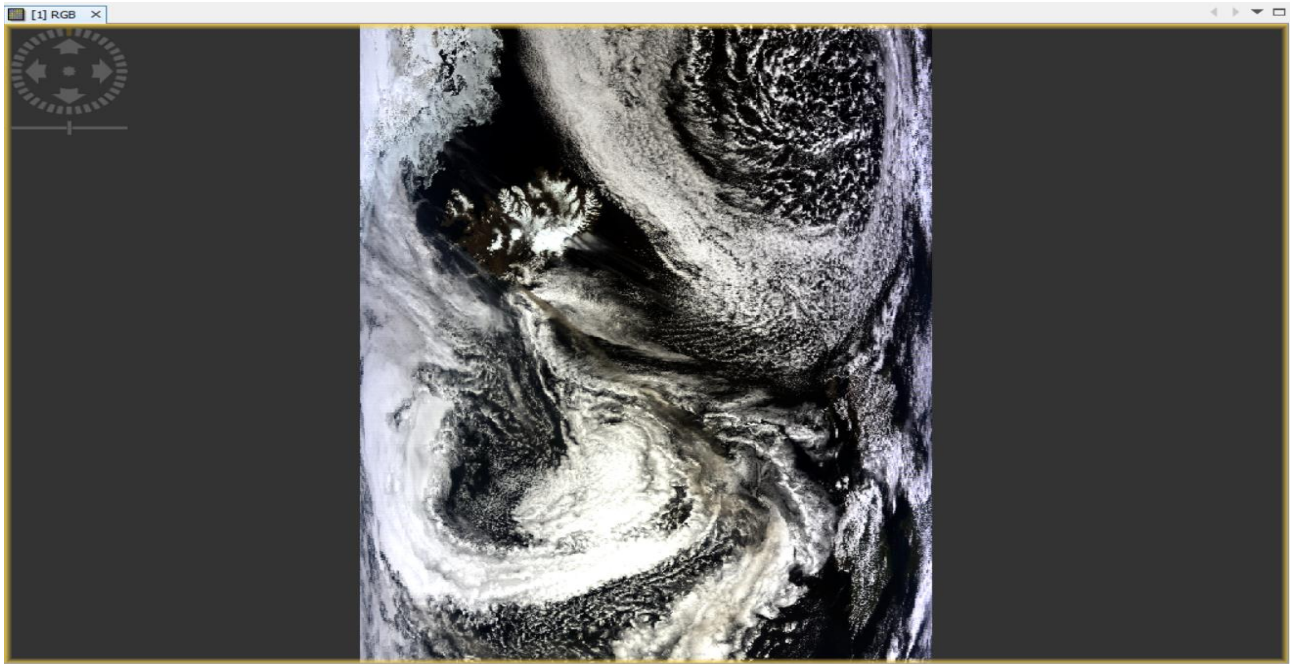

Figure 4: “visible” RGB (Red Green Blue) composite with MODIS data

6. Perform and display “virtual” RGB composite using SEVIRI data channels

For creating an RGB virtual composite image, we have used:

- IR8.7 (spectral band number 7) RED
- IR10.8 (spectral band number 9) GREEN
- IR12.0 (spectral band number 11) BLUE

Figure 5: "virtual" RGB (Red Green Blue) composite with SEVIRI data

7. Perform and display ash-cloud transects on SEVIRI RGB composite data

Using the SEVIRI imaginary (MSG_201005081200), we have created a path in the zone of the volcanic plume in order to analyse the ash clouds signatures.

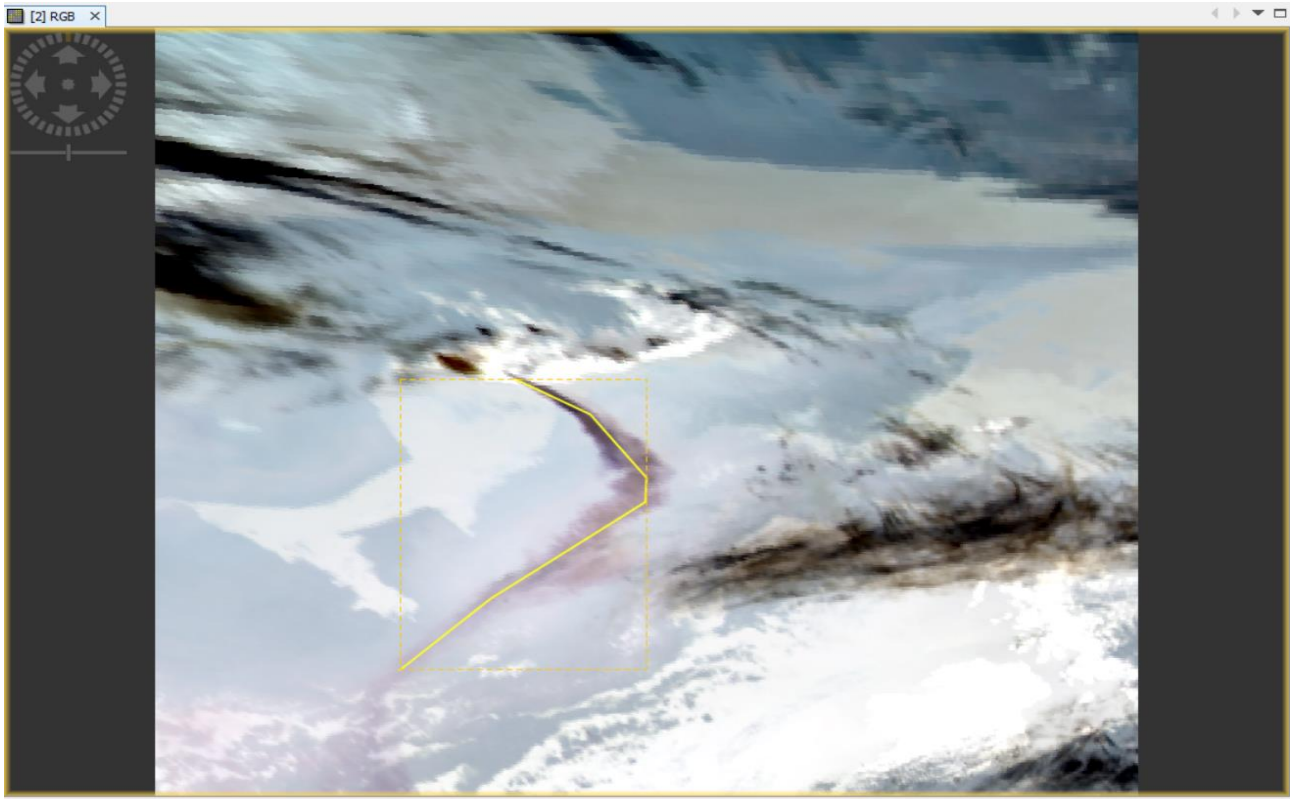

Figure 6: pixel path in the zone of volcanic plume using the first SEVIRI imaginary

Finally, we perform and display data analysis by profile tools obtaining the following image:

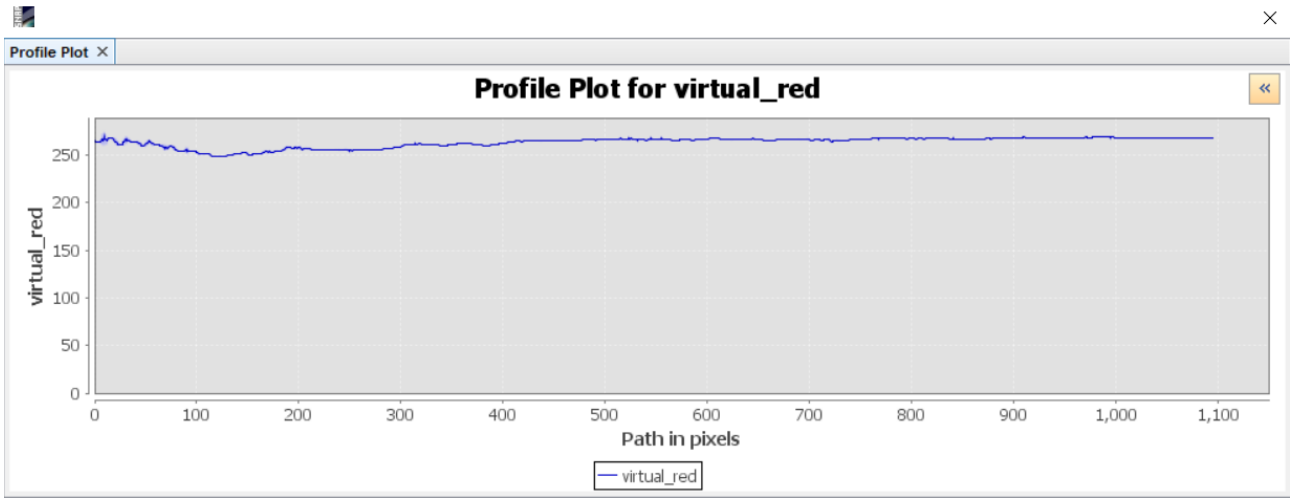

Figure 7: profile plot

8. Perform and display Brightness Temperature Difference (BTD) using SEVIRI data

Brightness Temperature Difference (BTD) is a basic detection technique exploiting the different behaviour of ash plumes in different spectral channels.

Most of the several BTDs – that can be defined to search for ash cloud signatures - involve using infrared channels. We have computed 3 different BTD:

a) BTD between IR_120 and IR_108 channels
b) BTD between IR_087 and IR_108 channels
c) BTD between IR_039 and IR_108 channels

a) BTD between IR_120 and IR_108 channels

Volcanic ash clouds which contain a high concentration of silicate particles can be detected using the brightness temperature difference between IR_120 and IR_108. This difference arises as an effect of the lower emissivity of silicate particles at 10.8 µm than at 12.0 µm. The resulting BTD of volcanic ash clouds will be positive and the BTD for ice clouds will be negative due to the lower emissivity at 12.0 µm.

Therefore, this method enables the discrimination among volcanic ash clouds and ice clouds.

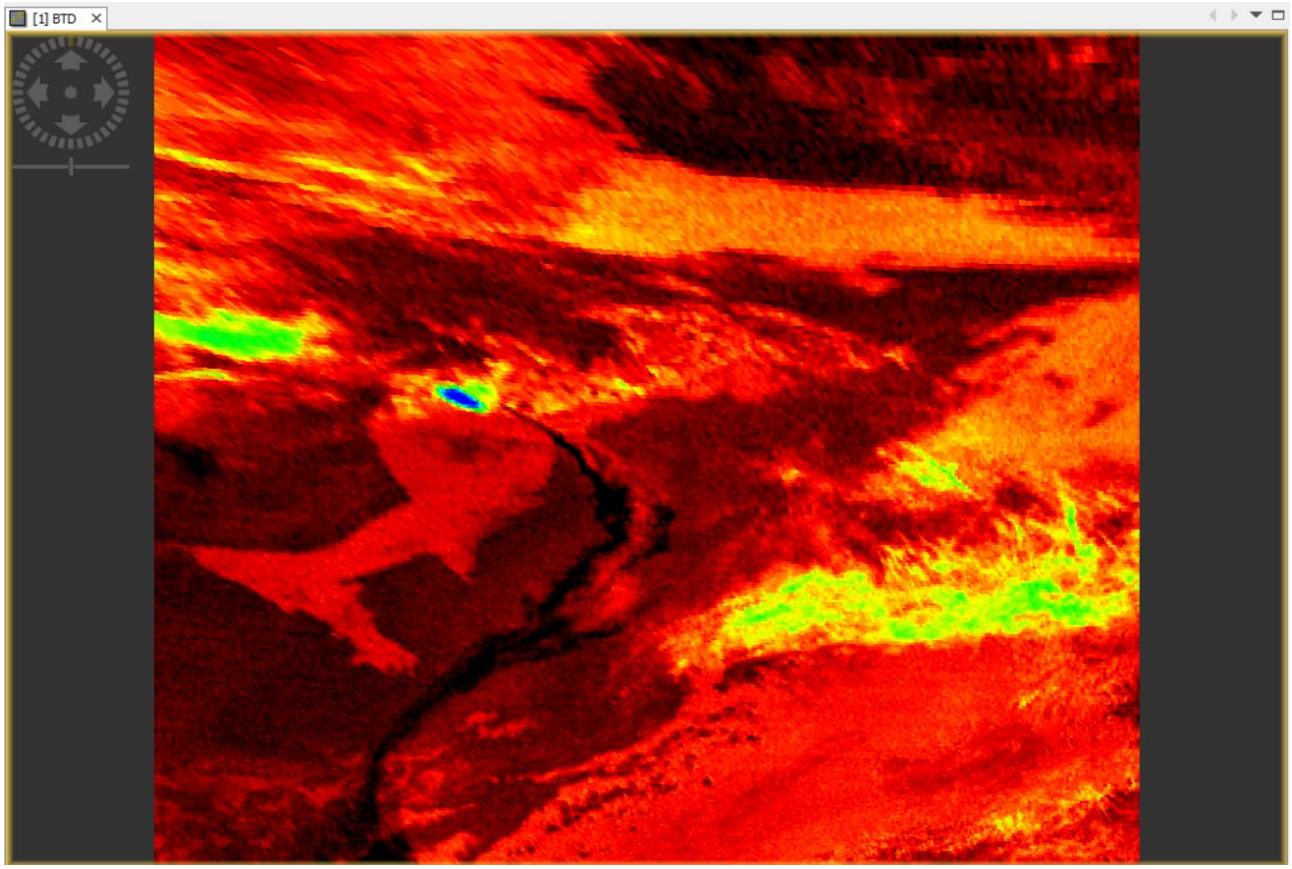

Figure 8: BTD between IR_120 and IR_108 channels

This BTD allows to discern between ice and ash clouds.

b) BTD between IR_087 and IR_108 channels

Apart from producing ash clouds volcanic eruptions release enormous amounts of gases. Volcanic plumes with high concentration of sulphur dioxide can be detected using the IR_087 channel.

The BTD IR_087 – IR_108 for SO_2 clouds its negative since, generally, $S0_2$ clouds are more transparent at IR_108 than at IR_87 due to the higher absorption at spectral ranges about 8.7µm. In contrast ice clouds are more transparent at IR8.7 than at IR10.8. As a result, observing ice clouds the BTD will be positive.

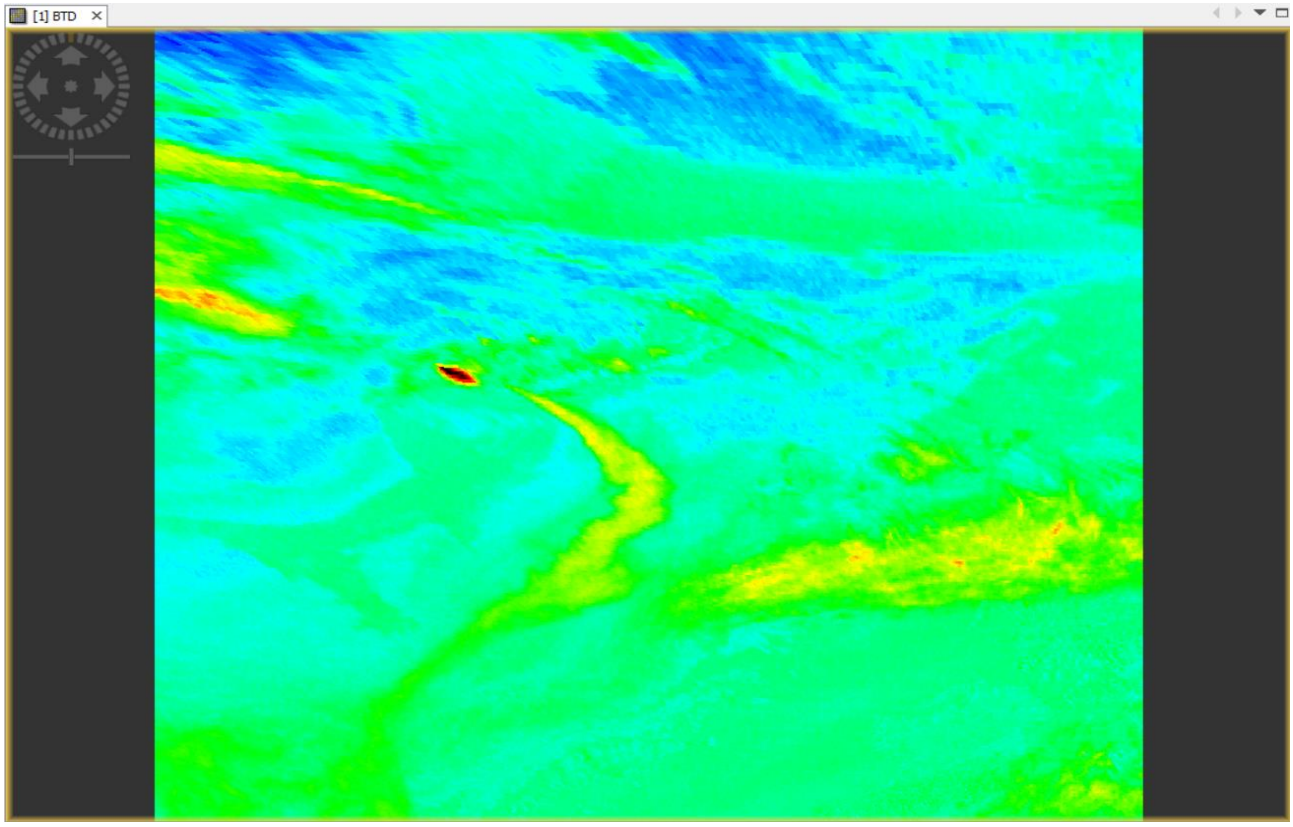

Figure 9: BTD between IR_087 and IR_108 channels

c) BTD between IR_039 and IR_108 channels

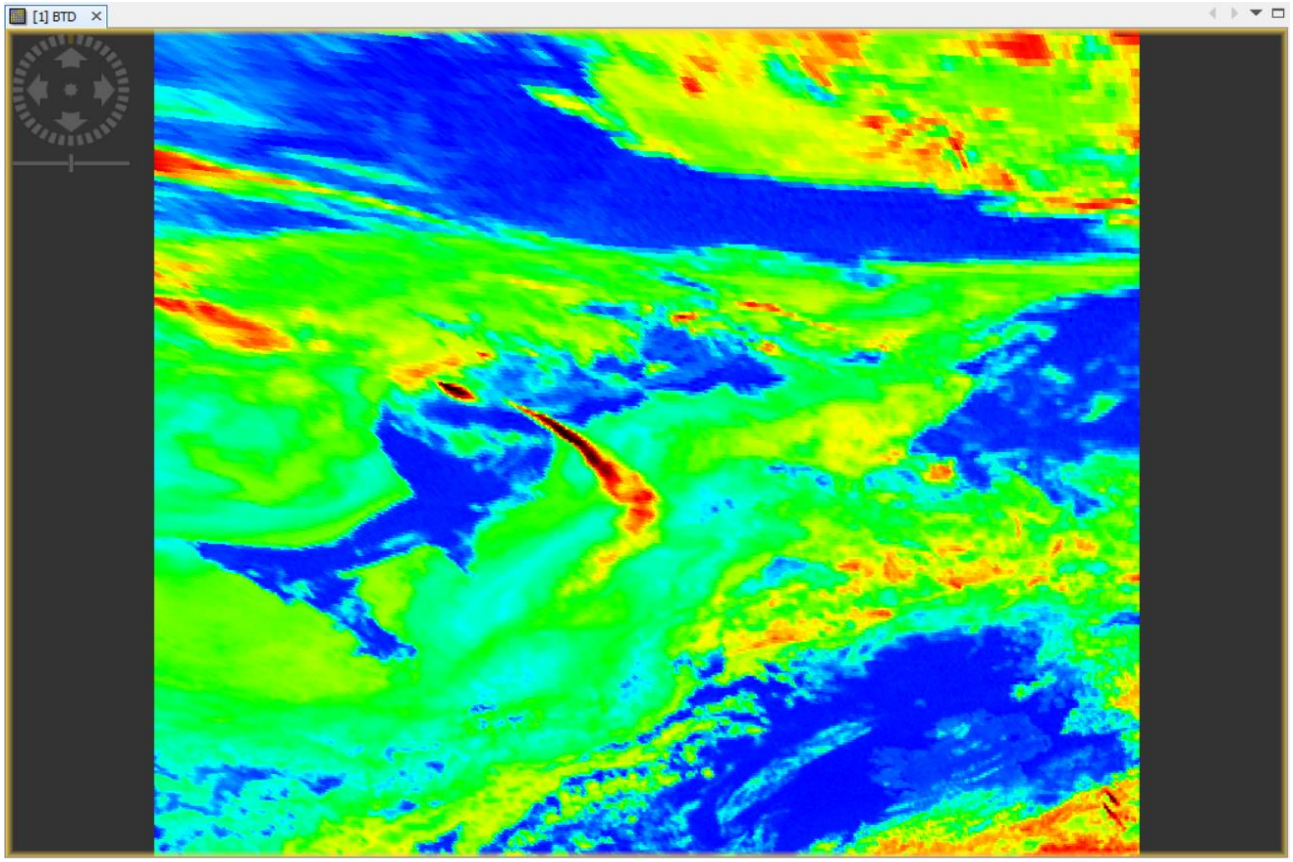

Figure 10: BTD between IR_039 and IR_108 channels

This BTD tends to be positive for ash clouds with a high concentration of sulphur dioxide and sulphate but, like the BTD between IR_087 and IR_108 channels, it does not allow to discern between ice and ash clouds.

9. Implement Volcanic Ash Detection Algorithm (VASD) using SNAP processing tools

The basic version of VASD consists in a binary algorithm, where there is a flag for ash cloud containing pixels and no flag for all the other classes of pixels. VASD uses a combination of the previously described tests, implementing the following conditions to detect an ash cloud:

$$\begin{cases} IR\_120 - IR\_108 > 0 \\ IR\_039 - IR\_108 > 0 \\ IR\_087 - IR\_108 > 0 \end{cases}$$

Another approach to define an alternative detection algorithm is to apply a different formula:

$$60 + 10 * (IR\_120 - IR\_108) + (IR\_039 - IR\_108) > 100$$

For implementing these formulas in SNAP, we need to go in: “Raster” ---> “Band Maths” and write them.

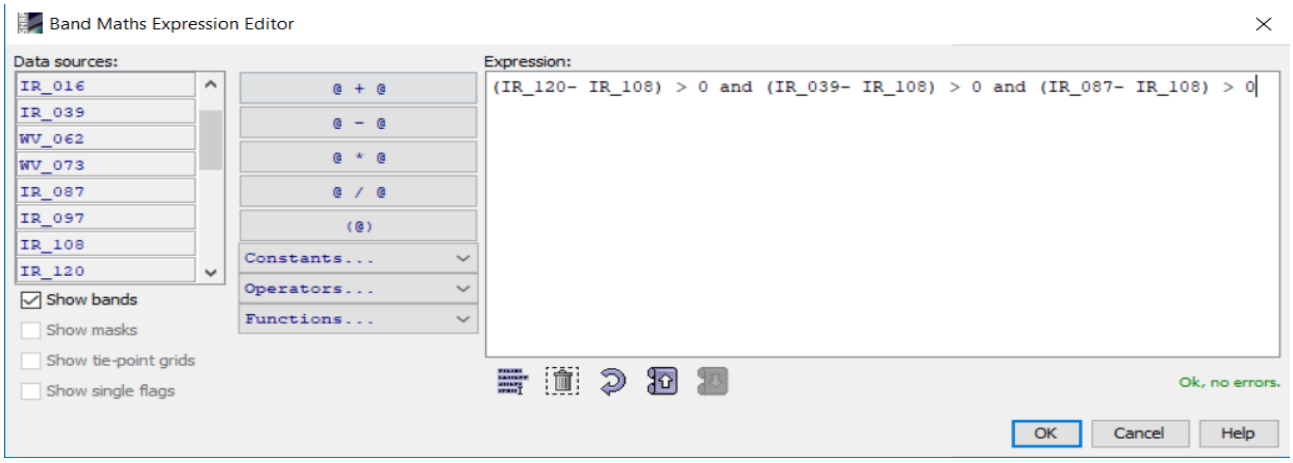

Figure 11: first implementation of VASD algorithm

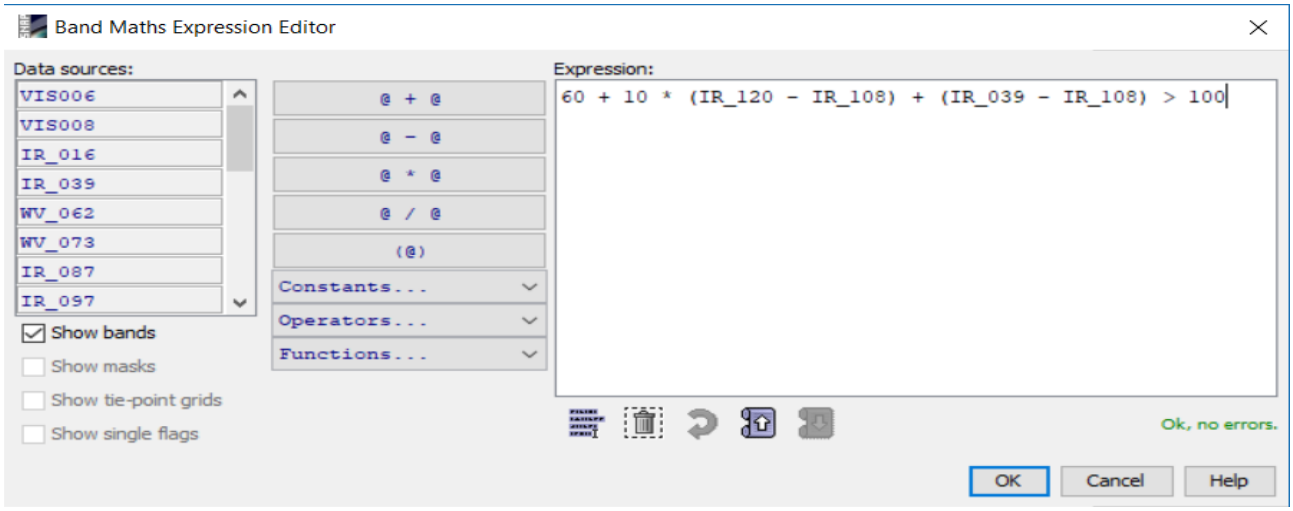

Figure 12: second implementation of VASD algorithm

10. Apply VASD (algorithm 1 and 2) and interpret their output results and differences

Applying the first VASD algorithm, we obtain the following result:

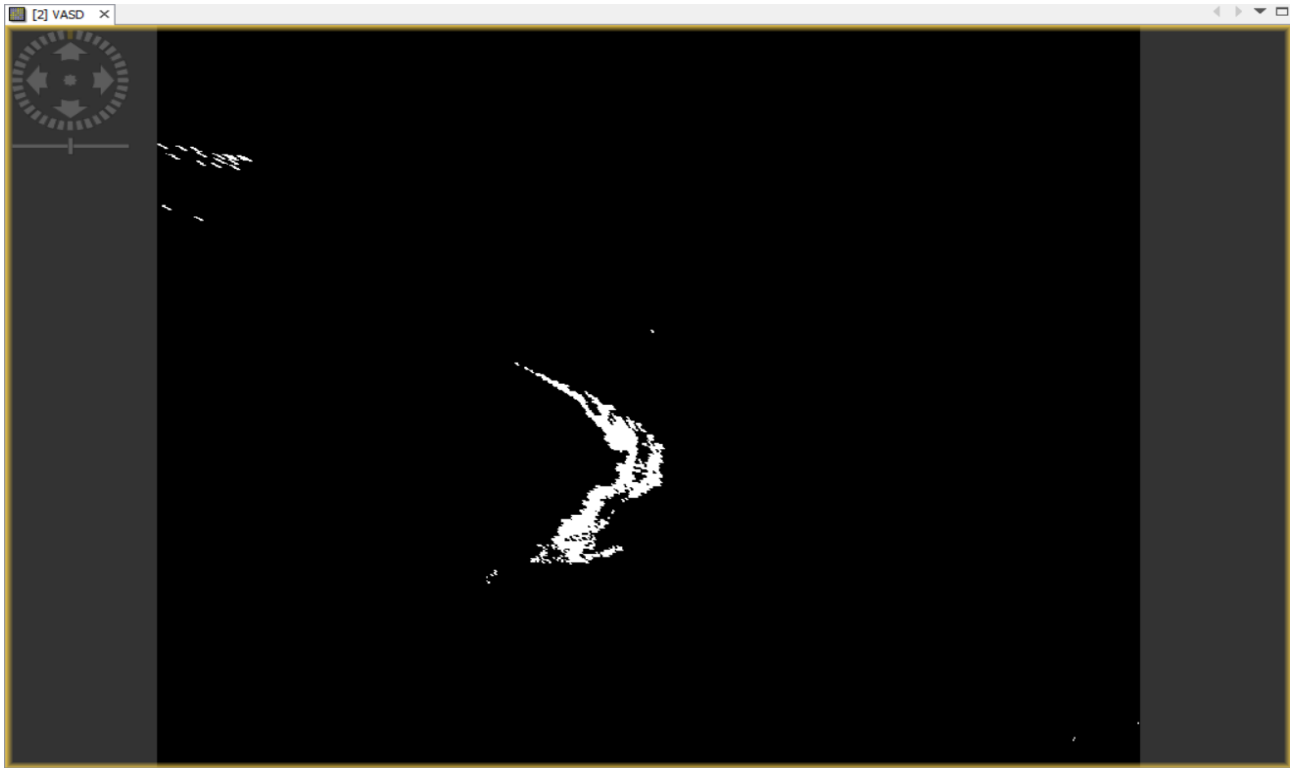

Figure 13: result derived from the first implementation of VASD algorithm

Applying the second VASD algorithm, we obtain the following result:

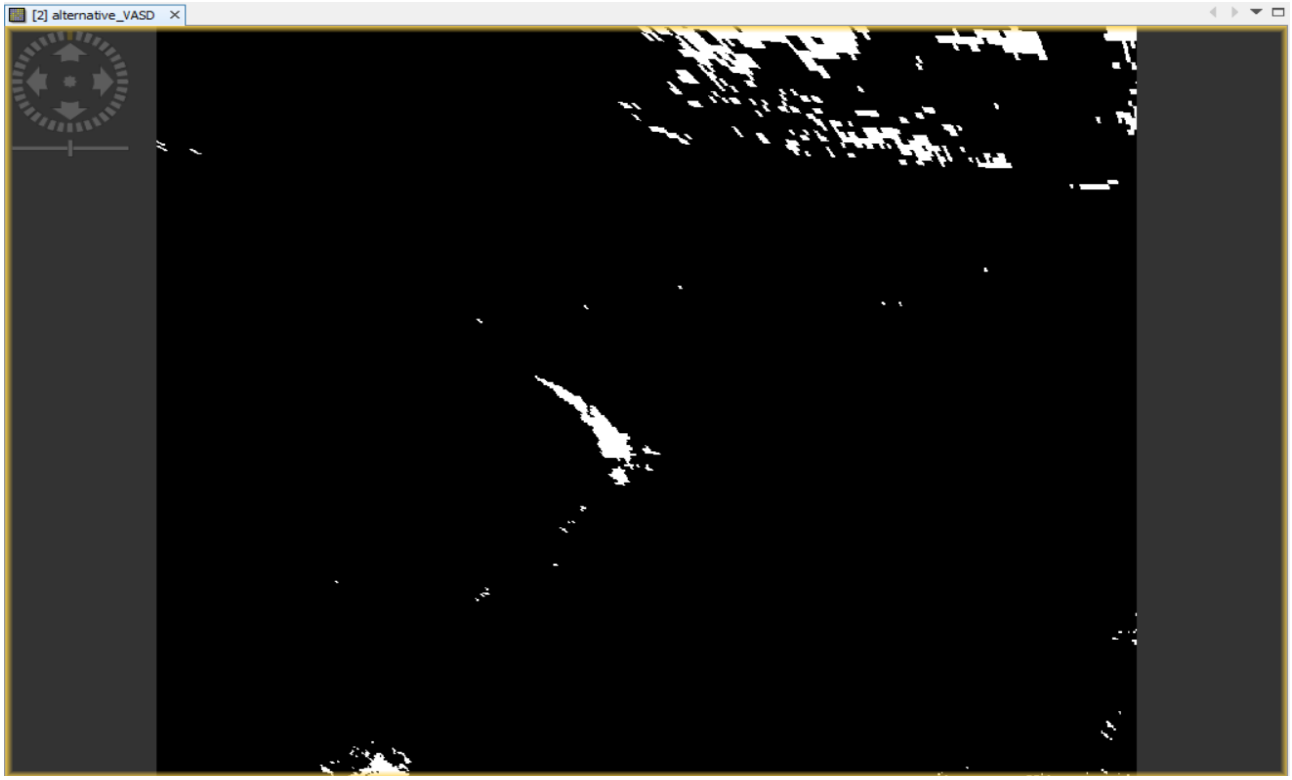

Figure 14: result derived from the second implementation of VASD algorithm

The first implementation of the VASD algorithm is less sensitive (i.e. higher number of false negatives – i.e. missed detections: pixels containing ash marked as if they are ash-free - or missed detection of ash pixels) with respect to the second implementation of the VASD algorithm, but in turn this results in a lower occurrence of false positives, i.e. false alarms: ash-free pixels marked as if they include ash.

11. **Develop and implement a TIR optical thickness retrieval algorithm by applying the no-scattering radiative transfer theory for a thermal homogeneous ash cloud layer noting that $T_B \leq T_0$ (you can use SNAP, Python/Matlab or R-language environment to implement the algorithm depending on its complexity)**

To implement a physically-based retrieval algorithm based on the simplified Radiative Transfer Model (RTM):

$$I_{\lambda sat}(\lambda) = \underbrace{t I_{\lambda srf}(\lambda)}_{\text{from surface}} + \underbrace{t(\lambda) w_s(\lambda) t(\lambda) I_{\lambda 0}(\lambda)}_{\text{from source and surface}} + \underbrace{t(\lambda) w_s(\lambda) I_{\lambda edwn}(\lambda)}_{\text{from medium and surface}} + \underbrace{I_{\lambda eupw}(\lambda)}_{\text{directly from medium}}$$

τ is the requested variable where satellite data are the inputs plus the unknown parameters T_{surf}, T_{cloud} and $e_{surf} = 1 - w_{surf}$.

The RTM can be further simplified by noting that unknown parameters can derived from ancillary sources:

- if we do the assumption of flat surface $w_{surf} \cong 0$, we obtain the following equation:

$$I_{\lambda sat}(\lambda) = \underbrace{t I_{\lambda srf}(\lambda)}_{\text{from surface}} + \underbrace{t(\lambda) w_s(\lambda) t(\lambda) I_{\lambda 0}(\lambda)}_{\text{from source and surface}} + \underbrace{t(\lambda) w_s(\lambda) I_{\lambda edwn}(\lambda)}_{\text{from medium and surface}} + \underbrace{I_{\lambda eupw}(\lambda)}_{\text{directly from medium}}$$

- if we do the assumption of the fully opaque atmosphere, we obtain the following equation:

$$I_{\lambda sat}(\lambda_{abs}) = I_{\lambda eupw}(\lambda_{abs})$$

Knowing that the optical thickness $\tau = k_{eo} L = \frac{k_{eo} H}{\sin\theta}$ and the transmittance $t(0, L) = e^{-k_{eo} L}$, substituting, we can obtain $t(0, L) = e^{-\tau}$. Moreover, for Rayleigh-Jeans (at MW) or Wien (at IR) approximation, the spectral radiance I_λ is related to the spectral brightness temperature $T_{\lambda B}$.

So, we can write the following equation:

$$I_{\lambda sat} \cong I_{BBcloud}(1 - t) \rightarrow I_{\lambda sat} \cong I_{BBcloud}(1 - e^{-\tau}) \rightarrow T_{\lambda Bsat} \cong T_{cloud}(1 - e^{-\tau})$$

$$\frac{T_{\lambda Bsat}}{T_{cloud}} \cong (1 - e^{-\tau}) \rightarrow e^{-\tau} = 1 - \frac{T_{\lambda Bsat}}{T_{cloud}} \rightarrow \tau = -\ln\left(1 - \frac{T_{\lambda Bsat}}{T_{cloud}}\right)$$

Since T_{cloud} is unknown, it can be estimated from the Wyoming RAOB database or can be estimated from the warmest radiance/TB pixel assumed it behaves like a black body. We estimate it using the second method (i.e. the warmest radiance/TB pixel assumed it behaves like a black body).

After that we estimate T_{cloud}, we are able to compute the optical thickness τ.

12. **Apply the TIR retrieval algorithm at 10800 nm and at 12000 nm to ash-cloud mask using SEVIRI data and interpret the output results. Note that thermodynamically data (useful to compute the Planck law) can be retrieved from http://weather.uwyo.edu/upperair/sounding.html.**

After the development and implementation of the TIR retrieval algorithm, we need to apply it at 10800 nm and at 12000 nm

- TIR retrieval algorithm to ash-cloud mask applied at 10800 nm

Applying the ash-cloud mask using SEVIRI data at 10800 nm, we obtain the following result:

Figure 15: ash-cloud mask applied at 10800 nm

Looking the colour manipulation tool window, we can see that the warmest radiance/TB pixel is 268.36 K

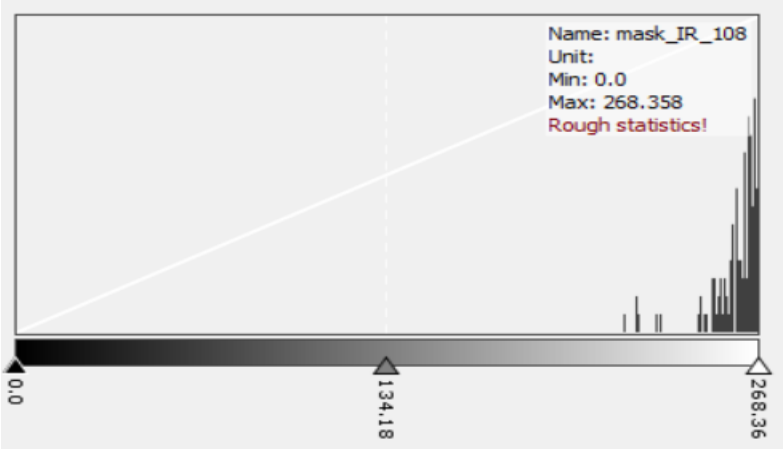

Table 2: colour manipulation tool window using the ash-cloud mask applied at 10800 nm

For computing $\tau = -\ln\left(1 - \frac{T_{\lambda \mathrm{Bsat}}}{T_{cloud}}\right)$, we substitute the values of $T_{\lambda \mathrm{Bsat}}$ and T_{cloud}, and we obtain:

$$\tau = -\ln\left(1 - \frac{mask\_IR\_108}{268.36}\right)$$

Applying the TIR retrieval algorithm at 10800 nm, we obtain the following result:

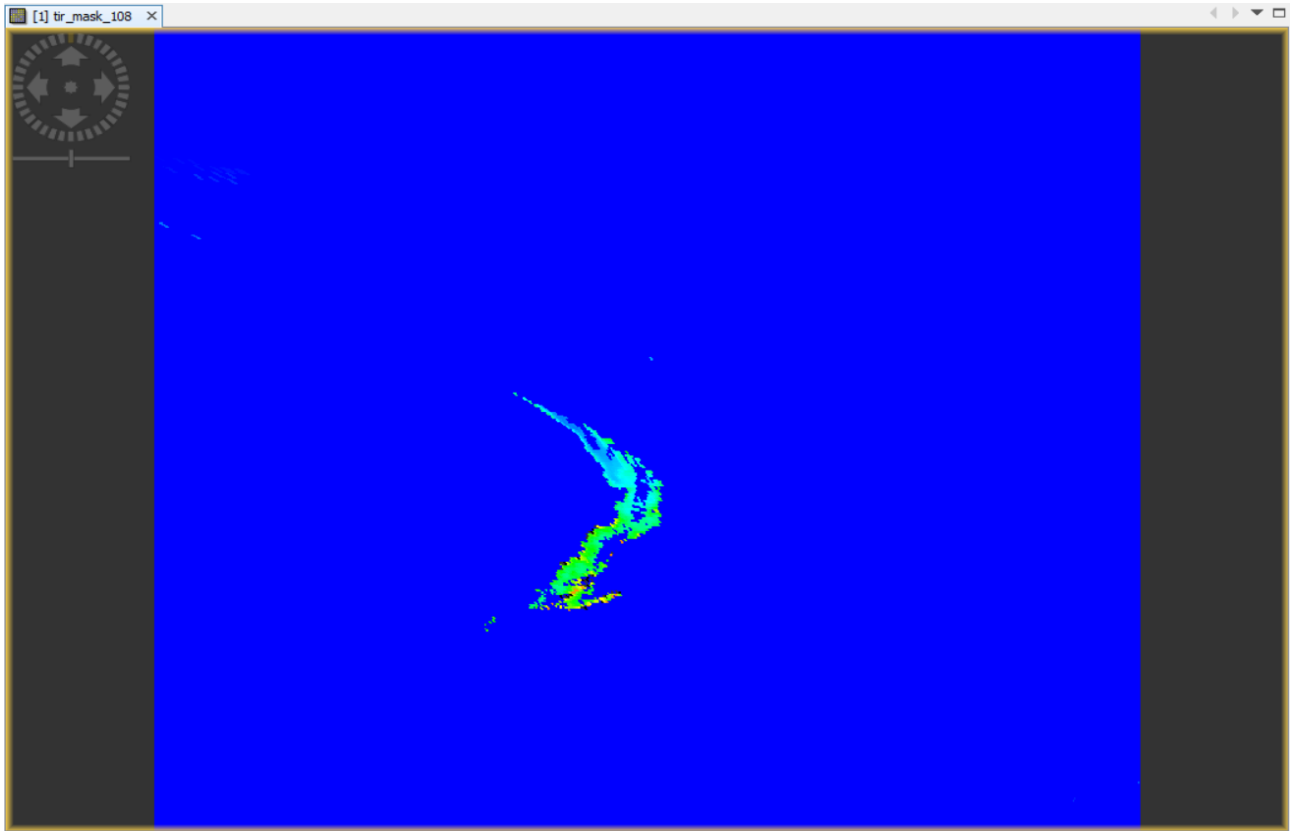

Figure 16: TIR retrieval algorithm to ash-cloud mask applied at 10800 nm

- TIR retrieval algorithm to ash-cloud mask applied at 12000 nm

Applying the ash-cloud mask using SEVIRI data at 12000 nm, we obtain the following result:

Figure 17: ash-cloud mask applied at 12000 nm

Looking the colour manipulation tool window, we can see that the warmest radiance/TB pixel is 270.31 K

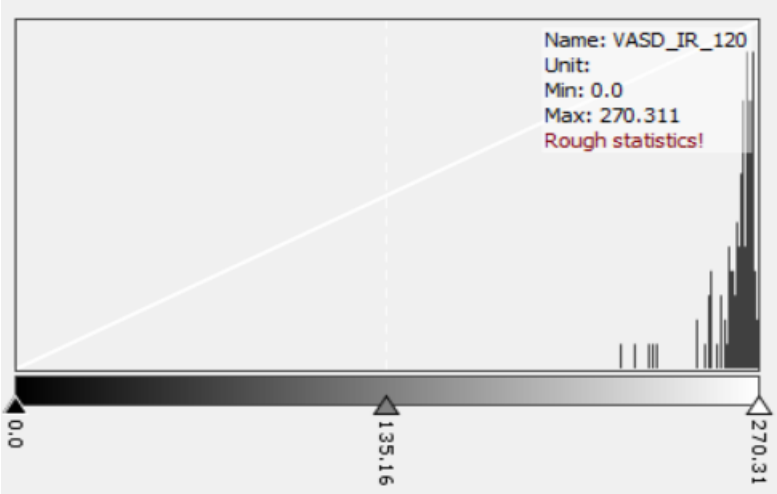

Table 3: colour manipulation tool window using the ash-cloud mask applied at 12000 nm

For computing $\tau = -\ln\left(1 - \frac{T_{\lambda \mathrm{Bsat}}}{T_{cloud}}\right)$, we substitute the values of $T_{\lambda \mathrm{Bsat}}$ and T_{cloud}, and we obtain:

$$\tau = -\ln\left(1 - \frac{mask\_IR\_120}{270.31}\right)$$

Applying the TIR retrieval algorithm at 12000 nm, we obtain the following result:

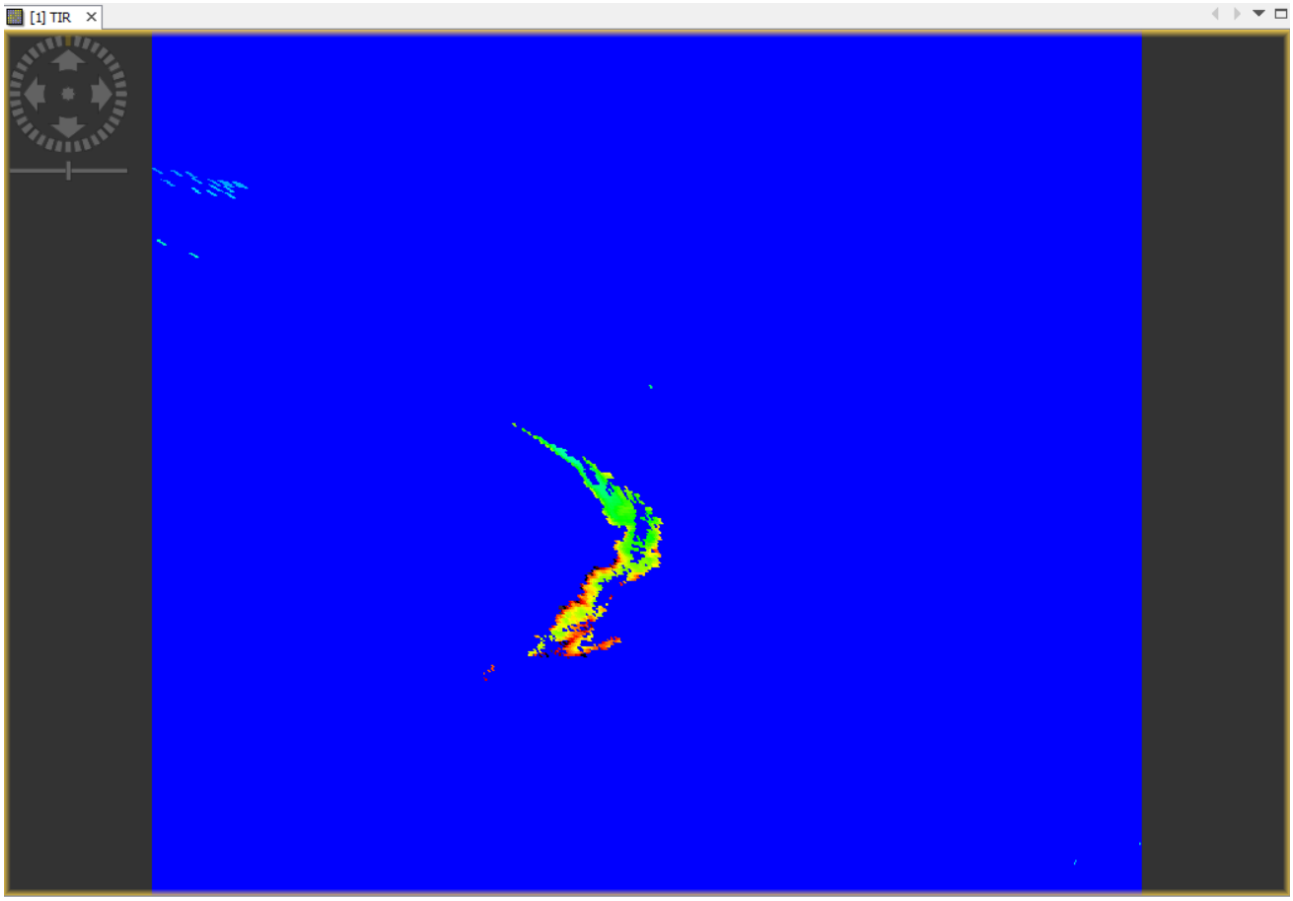

Figure 18: TIR retrieval algorithm to ash-cloud mask applied at 12000 nm

Applying the TIR retrieval algorithm to ash-cloud mask at 10800 nm, we can see that are a lot of pixels with low-medium intensity, while, applying the TIR retrieval algorithm to ash-cloud mask at 12000 nm, we can see that are a lot of pixels with medium-high intensity:

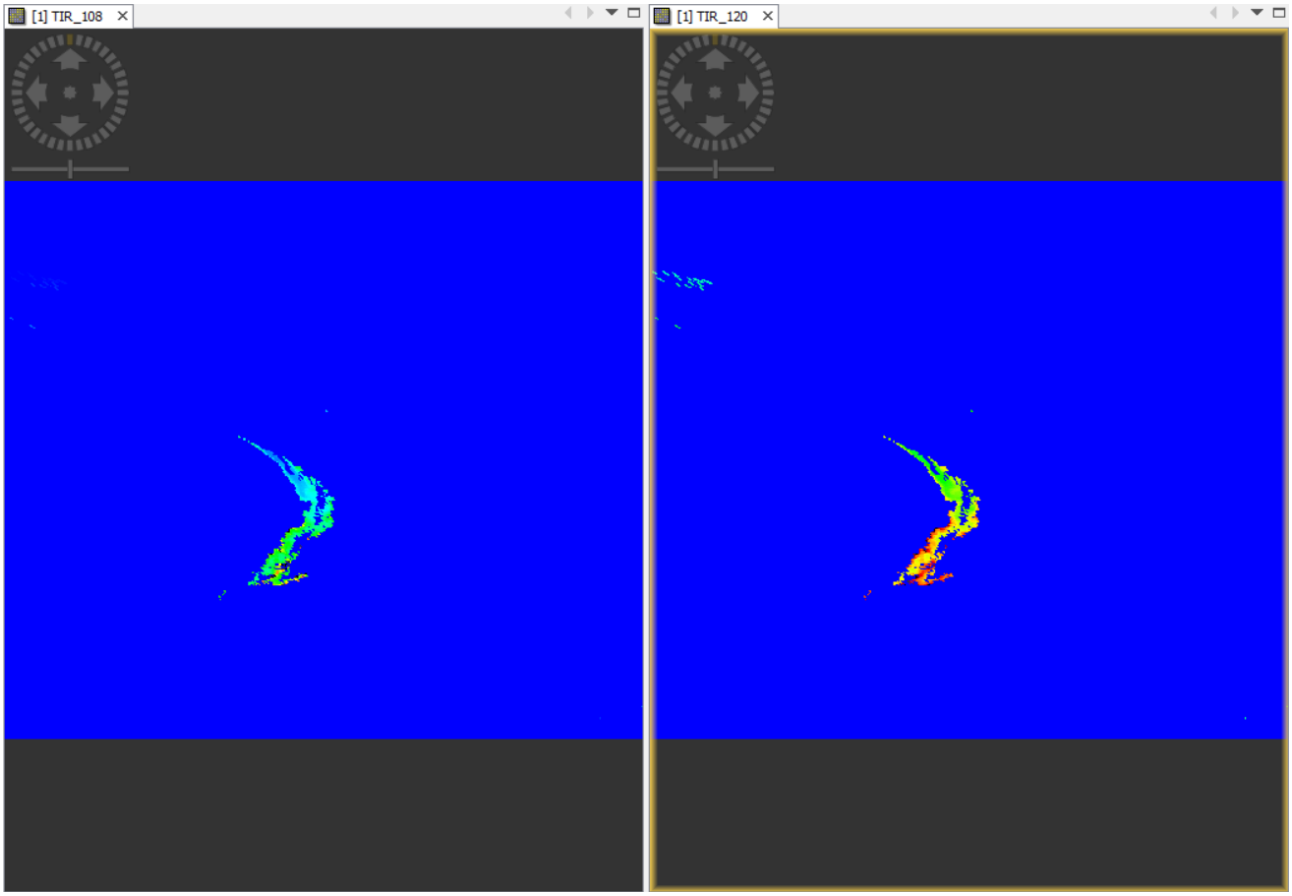

Figure 19: TIR retrieval algorithm to ash-cloud mask applied at 10800/12000 nm

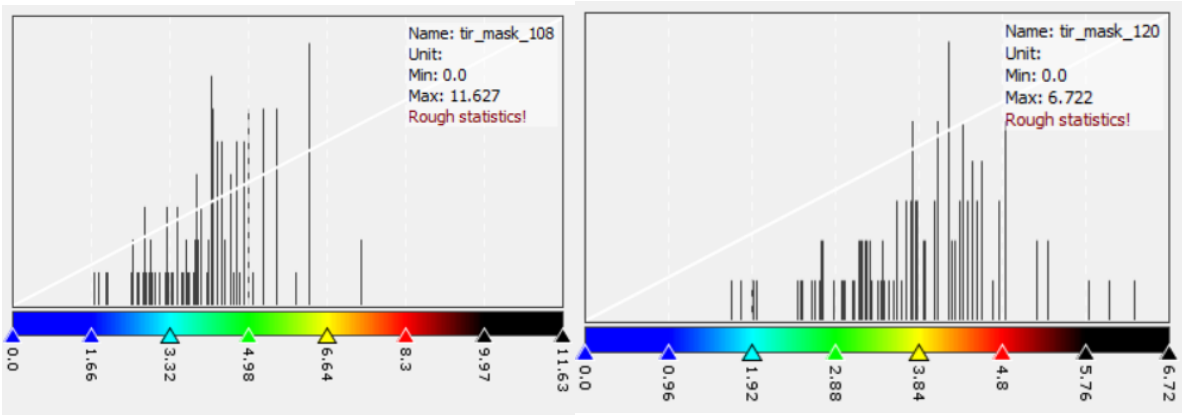

Figure 20: colour manipulation tool window using TIR retrieval algorithm to ash-cloud mask applied at 10800/12000 nm